Methylation of CAR is involved in the Suppression of CYP2C19 in HBV-associated Hepatocellular Carcinoma

Xiaojing Tang, Lele Ge, Zhongjian Chen, Sisi Kong, Wenhui Liu, Yingchun Xu, Su Zeng, Shuqing Chen

Institute of Drug Metabolism and Pharmaceutical Analysis, Zhejiang Province Key Laboratory of Anti-Cancer Drug Research, College of Pharmaceutical Sciences, Zhejiang University, Hangzhou, Zhejiang P. R. China (X.T., W.L., Y.X., S.Z., S.C.)

Department of Pharmacy, Sir Run Run Shaw Hospital, College of Medicine, Zhejiang University, Hangzhou, China (L.G.)

Department of Pharmacy, Zhejiang Cancer Hospital, Hangzhou, China (Z.C., S.K.)

Running title: Epigenetic Study of CYP2C19 in Hepatocellular Carcinoma

Corresponding author: Shuqing Chen

Address: Institute of Drug Metabolism and Pharmaceutical Analysis, Zhejiang Province Key Laboratory of Anti-Cancer Drug Research, College of Pharmaceutical Sciences, Zhejiang University, Hangzhou, Zhejiang P. R. China 310058

Tel: +86 571 88208411
Fax: +86 571 88208410
e-mail: chenshuqing@zju.edu.cn

Number of text pages: 36

Number of tables: 3

Number of figures: 7

Number of references: 25

Number of words in the Abstract: 196

Number of words in the Introduction: 590

Number of words in the Discussion: 1150

List of nonstandard abbreviations:

HCC, hepatocellular carcinoma; 5-aza-dC, 5-Aza-2'-Deoxycytidine; BSP, bisulfite sequencing PCR; MSP, methylation specific PCR; HBV, hepatitis B virus; HBsAg, hepatitis B surface antigen; HBcAb, hepatitis B core antibody; HCV, hepatitis C virus; CDS, coding DNA sequence; EGF, epidermal growth factor; EGFR, epidermal growth factor receptor; CAR, constitutive androstane receptor; HNF, hepatocyte nuclear factor; GR, glucocorticoid receptor; PXR, pregnane X receptor; SAM, S-adenosyl methionine.

Abstract

Hepatocellular carcinoma (HCC), one of the most dangerous malignancies with increasing incidence and high mortality rate, represents a major international health problem. The progression of HCC is known to involve a genome-wide alteration of epigenetic modifications, leading to aberrant gene expression patterns. The activity of CYP2C19, an important member of CYP450 superfamily, was reported to be compromised in HCC, but the underlying mechanism remains unclear. To understand if epigenetic modification in HCC is associated with CYP2C19 activity change, we evaluated the expression levels of CYP2C19 and its transcriptional factors by quantitative real-time PCR using mRNA extracted from both primary hepatocytes and paired tumor *vs* non-tumor liver tissues ofhepatitis B virus (HBV)-infected patients. DNA methylation was examined by bisulfite sequencing (BSP) and methylation specific PCR (MSP). Results indicated that CYP2C19 could be regulated by e-box methylation of constitutive androstane receptor (CAR). The decreased expression of CYP2C19 in tumorous tissues of HBV infected HCC patients is highly correlatedwith the suppressed expression and promoter hypermethylation of CAR. Our study demonstrated that aberrant CAR methylation is involved in the regulation of CYP2C19 in HBV-related HCC and it may play a role during liver tumorigenesis.

Introduction

Although tremendous endeavors have been made for a long time to fight against hepatocellular carcinoma (HCC), HCC still remains the fifth most prevalent cancer worldwide and is the third leading cause of cancer mortality up to now (Jemal et al., 2011). Hepatitis B virus (HBV) infection, Hepatitis C virus (HCV) infection and alcohol abuse are considered to be the main causes, among which HBV infection accounts for 60% of HCC in Chinese population. A recent report by World Health Organization estimated that 90 million people in China - almost 7% of Chinese population - are chronically infected with HBV.

Traditionally, HCC progression was considered as a gradual multistep process of normal cells evolving into tumor cells caused by mutations which lead to altered hepatocellular phenotypes (Thorgeirsson and Grisham, 2002; Lessel et al., 2014). However, evidence accumulated in the past few decades suggest that altered epigenetic modifications also play a pivotal role in HCC development (Nishida and Goel, 2011). DNA methylation, which refers to the addition of a methyl group to the cytosine within a CpG dinucleotide, is the most intensively studied epigenetic mechanism in mammals. It has been reported that the cancerous tissues in HCC possess a unique methylation landscape which differs from adjacent tissues. In HCC, the methylome feature is roughly characterized by global hypomethylation and gene-specific DNA hypermethylation, which contribute to genomic instability and inactivation of tumor-suppressor genes, respectively (Herceg and Paliwal, 2011). Since advanced HCC is highly lethal and incurable, there is an urgent need for

understanding the tumorigenesis process as well as searching for new diagnostic biomarkers and novel therapeutic targets.

CYP2C19 is one of the most important members of CYP450 superfamily and is responsible for the metabolism of a variety of clinical important drugs like mephenytoin, diazepam and some barbitals (Griskevicius et al., 2003). The genetic polymorphisms of CYP2C19 have been well studied. Individuals can be divided into extensive metabolizers (EMs), intermediate metabolizers (IMs), poor metabolizers (PMs) and ultra-rapid metabolizers (UMs) based on the catalytic capacity of the enzyme, which is largely dependent on different alleles the individuals are carrying (Uppugunduri et al., 2012). The regulatory mechanism of CYP2C19 is currently characterized by several nuclear receptors and transcriptional factors including CAR, PXR, GRα and HNF-3γ, among which CAR appears to play a central role and has strong associationwith the basal expression level of CYP2C19 (Wortham et al., 2007). It has been predicted that epigenetic might also play a role in the regulation of CYP2C19 and there exist some CpG sites in the 5'-flanking region of CYP2C19 gene, but their functional importance remains to be further elucidated (Ingelman-Sundberg et al., 2007).

The expression of CYP2C19 is reported to be decreased in advanced cancers including breast cancer, lung cancer, as well as HCC, which is also accompanied by comprised enzymatic activity (Helsby et al., 2008; Tsunedomi et al., 2005). However, regardless of the extensive effort to investigate the underlying mechanism over the past years, the altered expression of CYP2C19 in HCC does not appear to be fully

accounted by either known polymorphisms, or inflammatory factors, or growth

hormones (Helsby et al., 2008). The aim of this study is to investigate the possible

epigenetic mechanism in the decreased expression of CYP2C19 in HBV infected

HCC. Since CYP2C19 is also important in the disposition of a number of

chemotherapeutic agents, including cyclophosphamide, thalidomide and bortezomib,

elucidating the epigenetic modulation of CYP2C19 might also help understand and

predict the chemotherapy outcome for HCC patients.

Materials and Methods

Cell Culture and Tissue Samples

HepG2 and HEK293 cells were grown in DMEM medium (Life Technologies, Carlsbad, CA), supplemented with 10% FBS (Life Technologies, Carlsbad, CA) and 1% PEST (Life Technologies, Carlsbad, CA), at 37℃ with 5% CO_2. HK2 cells were grown in DMEM/F-12 medium (Life Technologies, Carlsbad, CA) supplemented with 18% FBS at 37℃ with 5% CO. Cryopreserved primary hepatocytes (RILD Research Institute for Liver Disease, Shanghai, China) from one male and one female donor (Supplemental Table 1) were plated in InVitroGRO™ CP Medium (BioreclamationIVT, Baltimore, MD) at 37℃ with 5% CO_2 before drug incubation. 2 replicates were conducted for each donor.

Thirty pairs of tumorous and adjacent liver tissues were obtained from fresh surgical specimen of HBV infected HCC patients (HBV DNA>1000copies/ml or HBsAg and HBcAb test positive) and were then stored in liquid nitrogen before use. The selected patients did not receive any radiotherapy or chemotherapy before. Tissues were obtained from Zhejiang Cancer Hospital. Information of liver species is provided as Supplemental Table 2. The research protocol has been carried out in accordance with the Declaration of Helsinki and was approved by the Ethics Committee of Zhejiang Cancer Hospital.

Treatment of Primary Hepatocytes with 5-aza-dC

Primary hepatocytes were seeded at a density of 5×10^5 cells/ml in collagen-coated

6-well plates (Life Technologies, Carlsbad, CA) with *InVitro*GRO™ CP Medium (BioreclamationIVT, Baltimore, MD). Medium was changed the next day to remove the unattached cells. After 24h of plating, drug incubation started with 1μM and 2μM 5-aza-dC (Sigma, St. Louis, MO) (Christman, 2002) in *InVitro*GRO™ HI Medium supplemented with 25ng/ml EGF (Sigma, St. Louis, MO) to stimulate proliferation. Control group was treated with 0.1% DMSO. Medium was changed every other day. Cells were harvested after 5 days treatment for DNA and RNA isolation.

Semi-quantitative Real-Time PCR

mRNA was extracted from tissue samples and cultured cells using the RNeasy Mini Kit (Qiagen, Valenica, CA). 500ng mRNA was used in reverse transcribed PCR reaction performed with PrimeScript RT reagents Kit (Takara, Tokyo, Japan) and thenquantitative real-time PCR was performed using the SYBR$^®$ Premix Ex Taq™ II (Takara, Tokyo, Japan) and the StepOnePlus™ System (Applied Biosystems, Foster City, CA). Primers for quantitative real-time PCR are listed in Table 1. Relative quantitation of gene expression was calculated with the $2^{-\Delta\Delta Ct}$ method as described previously (Schmittgen and Livak, 2008).

Table 1.

DNA Methylation Analysis

Genomic DNA from tissue samples or cells was isolated using the DNeasy Blood &Tissue Kit (Qiagen, Valenica, CA). DNA was considered qualified with a ratio of

absorbance at 260nm and 280nm (A260/A280) between 1.7 and 1.9. Samples were stored in elution buffer at -80°C before use.

Sodium bisulfite modification of DNA samples was conducted using an EZ DNA Methylation™-Gold Kit (Zymo, Orange, CA). The location of all CpG sequences examined in this study is shown in Figure 1. PCR amplification was done with rTaq polymerase (Takara, Tokyo, Japan) in a 50μl reaction mixture with 2μl modified DNA as template. It starts with 10 cycles of touchdown PCR of 30s at 94℃, 30s at 60℃ to 55℃ (-0.5℃ per cycle), and then 45s at 72℃ and 30 cycles of 30s at 94℃, 30s at 55℃, 45s at 72℃, and finally an extension of 10min at 72℃. Amplicons were then purified and subcloned into pMD18-T vector (Takara, Tokyo, Japan) according to manufacturer's instruction. Ligation products were transformed into E. coli DH5α cells and 10-15 random colonies with recombinant plasmids were subjected to Sanger sequencing (Sangon, Shanghai, China).

Methylation-specific PCR was also conducted using the modified DNA as template. The followingtouchdown PCR program was applied: 10 cycles of touchdown PCR of 30s at 94℃, 30s at 58℃ to 53℃ (-0.5℃ per cycle), 20s at 72℃ and 25 cycles of 30s at 94℃, 30s at 53℃, 20s at 72℃, followed by a final extension of 10min at 72℃. 10μl PCR products were shown on a 2% agarose gel containing ethidium bromide. Primers for methylation analysis are listed in table 2.

Figure 1.

Table 2.

Plasmids Construction

pCpGL-CYP2C19 (-1977~+64), pCpGL-CAR-CGI (-1446~+1971), pCpGL-CAR-2E

(+175~+1971) and pCpGL-CAR-1E (+384~+1971) were constructed with a CpG-free

luciferase reporter vector named pCpGL-basic (Fig. 2A) (Klug and Rehli, 2006).

pCpGL-CYP2C19 contains a ~2.0kb sequence of the 5'-flanking promoter region of

CYP2C19. pCpGL-CAR-CGI contains a ~3.5kb sequence with a CpG island on the

5'-flanking region and both e-box binding sites close to transcription start site and

translation start site of CAR, respectively. In pCpGL-CAR-2E, the CpG island region

is deleted from the sequence of pCpGL-CAR-CGI, while in pCpGL-CAR-1E, another

~200bp sequence which contains the first e-box binding site was deleted. Additionally,

a full-length CAR CDS amplified from mRNA (primers CDS-F/R) was ligated with

the 5'-flanking region as well as the untranslated exon 1 and intron 1 (amplified by

primers Flanking-F/R) by overlap PCR. The ~3kb ligated fragment was then inserted

into a CpG-free expression vector, pCpGfree-mcs (Fig. 2B) (InvivoGen, San Diego,

CA), to construct pCpGfree-CAR. Primers used for plasmids construction are listed in

Table 3. All constructs were confirmed by Sanger sequencing (Sangon, Shanghai,

China).

Figure 2.

Table 3.

In vitro **Methylation of Plasmid DNA**

Plasmids were methylated using M. SssI (NEB, Beverly, MA) according to

manufacturer's instruction. 2μg plasmid DNA was incubated in a 40μl volume with

2μl (4U /μl) Sss I and 160μM SAM at 37℃ for 6 hours. The control group of plasmid

also underwent the same incubation, but in the absence of Sss I. The reaction was

stopped by heating at 65°C for 20 minutes. Both methylated and control group of

plasmid DNA was purified with Axygen PCR Clean-up Kit (Axygen, Hangzhou,

China).

Transient Transfection Assay

HepG2, HEK293 or HK2 cells were seeded in 24-well plates at the density of 2.5×10^5

/ml. The transient transfection was carried out using Lipofectamine2000 (Life

Technologies, Carlsbad, CA) when cells have reached 70~80% confluence. Reporter

plasmids and expression plasmids were transfected at 500ng and 250ng per well,

respectively, with 50ng pRL-TK per well as internal control. Medium was refreshed 6

hours after transfection. Luciferase activity was assessed using the Dual-Luciferase

Reporter Assay System (Promega, Madison, WI) 48 hours post transfection.

Statistical Analysis

qPCR results were shown as $2^{-\Delta\Delta Ct}$ using GAPDH as housekeeping gene. The

methylation percentage of BSP analysis was calculated as the number of methylated

cytosines divided by the total number of cytosines on the CpG site in all amplicons.

The methylation percentage of a sequence was determined as the average percentage

of all CpG sites within this region. Comparison of methylation percentage and mRNA

expression between groups was analyzed by Paired Student's t test using GraphPad

Prism 5.0 (GraphPad, San Diego, CA) software. The correlation between CYP2C19

and CAR expression was determined by Pearson correlation. Difference or correlation

is considered statistically significant at the level of $*p < 0.05$, $**p < 0.01$ and $***p < 0.001$.

Results

Increased CYP2C19 and CAR mRNA in Primary Hepatocytes after 5-aza-dC

Treatment

In order to determine whether DNA methylation is a potential mechanism of CYP2C19 regulation in the liver, a DNA methyltransferase inhibitor, 5-aza-dC, was applied to the primary cultures of human hepatocytes. Quantitative real-time PCR analysis revealed an increase of CYP2C19 and CAR expression in a dose-dependent manner, while other transcriptional factors were not significantly affected (Fig. 3). To investigate if it was the demethylation that led to the elevated expression level of CYP2C19 and CAR in primary hepatocytes, BSP was performed on the promoter regions as shown in Figure 1. BSP results revealed a moderate methylation frequency on the CpG-poor promoter of CYP2C19 (52.5%) as well as the two e-box binding sites on CAR (50% and 47.5%). After 5-aza-dC treatment, the methylation frequency of these three regions decreased to 38.3%, 13.3% and 42.5%, respectively (Fig. 4A-4C). The CpG island on CAR promoter, which was highly methylated (92.5%), also showed a decreased methylation frequency (72.5%) after exposure to 5-aza-dC (Fig. 4D). BSP results showed an overall decreased DNA methylation level on the promoter of CYP2C19 and CAR after the treatment of 5-aza-dC. These results suggested that DNA methylation is a regulatory mechanism of CYP2C19 in liver, in which CAR might also be involved.

Figure 3.

Figure 4.

Decreased mRNA Expression of CYP2C19 and CAR in Tumorous Tissues

The expression of CYP2C19 and CAR in tumorous and adjacent tissues is shown as grouped column scatter with mean ± S.E. in Figure 5A. The average expression of CYP2C19 in tumorous tissues (0.39 ± 0.20) was significantly decreased compared with the normal tissues (2.4 ± 0.40, ***$p < 0.001$). In addition, the average expression of CAR also decreased significantly (0.40 ± 0.085 *vs* 1.40 ± 0.15, ***$p < 0.001$). The alterations of expression level of CYP2C19 and CAR were correlated with a Pearson correlation coefficient of 0.31 (R^2=0.09, *$p < 0.05$) (Fig. 5C).

Figure 5.

Elevated Methylation Level of CpG Sites on CAR Promoter in Tumorous Tissues

BSP analysis of segment 5 on CAR was performed using DNA from paired tumor and adjacent tissue samples. Representative BSP results are shown in Figure 6A and corresponding relative mRNA expression were shown in Figure 5B. Clearly, in BSP analysis, CpG 3, CpG 5 and CpG 6 in segment 5 around the transcription start site of CAR were in a higher methylated status in tumorous tissue compared with adjacent tissue. Among these three sites, CpG 3 is a potential e-box binding site, while CpG 5 and 6 are two adjacent CpG sites 121 bp downstream of CpG 3. In addition, MSP within segment 5 also revealed a higher methylation level in tumorous tissues (Fig. 6B). Interestingly, in the case of sample 246564, the expression level of CAR and CYP2C19 were increased while methylation status was decreased in tumorous tissues

(Fig. 6A). No significant methylation difference was detected between tumorous and

adjacent tissues in the other BSP analyzed segments (data not shown).

Figure 6.

In vitro Methylation on CAR Promoter Leads to Decreased CAR Mediated

CYP2C19 Expression in HepG2 Cells

The results of dual-luciferase reporter assay showed that the CpG-poor 2kb promoter

of CYP2C19 was not affected by methylation (Fig. 7A, 7C, 7D) in all tested cell lines,

suggesting that these sporadic CpG sites are irrelevant to the methylation mechanism.

The unmethylated pCpGL-CAR-CGI was 2.5-fold higher in relative luciferase

activity compared to the methylated group in HepG2 cells. This fold change sustained

after the deletion of the CpG island as shown by the unmethylated *vs* methylated

pCpGL-CAR-2E (2.2 fold), but was greatly reduced after deletion of the 200bp

fragment containing the e-box binding site near the transcription start site (in the first

intron), indicating that this e-box binding site was essential in the methylation

regulating mechanism of CAR, whereas the e-box close to the translation start site

was not involved. However, no difference between the methylated and unmethylated

group was found in HK2 or HEK293 cells (Fig. 7C, 7D).

To explore if the methylation-mediated decrease of CAR could exert an effect on

CYP2C19 expression, either methylated or unmethylated pCpGfree-CAR was

co-transfected with pCpGL-CYP2C19 in HepG2 cells. A 2.3-fold higher luciferase

activity was observed in the unmethylated pCpGfree-CAR group (Fig. 7B), which

further supported that CYP2C19 could be suppressed through the hypermethylation

caused decrease of CAR expression.

Figure 7.

Discussion

HBV infection is still a key issue in China's health care according to the *World Cancer Report* published by the WHO in 2014. The HBV-induced hepatocarcinogenesis includes proteomic disruption, viral integrations and aberrant epigenetic modifications (Ji et al., 2014). In the present study, we demonstrated that DNA de-methylation led to elevated CAR and CYP2C19 expression in primary hepatocytes. This finding suggests that DNA methylation is a potential mechanism of CAR and CYP2C19 regulation in the liver. This notion is further supported by the suppressed CAR and CYP2C19 expression in Chinese HBV-related HCC patients.

Since CAR is a member of the nuclear receptor superfamily and a central modulator of oxidative and conjugative enzymes and transporters that are involved in drug disposition and metabolism, it is conceivable that the suppression of CAR plays an important role in the altered expression of CYP2C19 and possibly other targeting drug metabolism genes. CYPs participate in the activation and metabolism of a large number of chemotherapeutic agents such as docetaxel (Shou et al., 1998) and cyclophosphamide (Griskevicius et al., 2003). Thus, CAR suppression mediated by hypermethylation may lead to disturbance of the drug metabolizing system. Therefore, the methylation status of CAR might serve as a biomarker of altered pharmacokinetics. Indeed, it has been confirmed in other studies that several CAR-regulating CYP genes were also suppressed along with the decreased CAR expression in end-stage HCC (Chen et al., 2014), but no significant decrease of CAR and related CYP genes was found in HBV cirrhosis samples. This finding suggested that the sharp decline in the

expression of these genes might occur when liver cirrhosis evolves into carcinoma. However, our result only offered a Pearson correlation coefficient of 0.31 between the CYP2C19 and CAR expression in contrast to a stronger correlation (Pearson correlation coefficient of 0.693) observed in healthy liver samples (Wortham et al., 2007). Since it has been demonstrated that down-regulation of metabolism related genes is preferentially linked with HBV-related HCC, rather than HCV-related HCC (Okabe et al, 2001; Iizuka et al, 2001), it is possible that the virus itself might have direct impact on the expression of certain genes. Furthermore, as the regulation of CYP2C19 is a complicated network contributed by multiple factors, the effect of CAR might be diluted *in vivo*. Actually, more and more mechanisms have been discovered in recent years. One example of the epigenetic mechanism is the participation of hsa-miR-29a-3p in the regulation of CYP2C19 in liver cells (Yu et al., 2015). miRNA may also participate in disrupting the correlation between CAR mRNA and protein level, thus leads to the poor correlation between CAR and CYP2C19 mRNA level. Further study is warranted to build a comprehensive map of how CYP2C19 is regulated in HCC.

Since there was a 2-fold decrease in luciferase activity after the deletion of 200 bp sequence containing the e-box at the first intron as indicated in the reporter gene assay, this sequence may act as an enhancer element of CAR. This hypothesis warrants further investigation. We performed the same *in vitro* methylation and reporter gene assay in three cell lines, HepG2, HEK293 and HK2. Interestingly, only HepG2 showed decreased luciferase activity in methylated pCpGL-CAR-2E. No difference

between the methylated and unmethylated pCpGL-CAR-2E was detected in either HEK293 or HK2. The results indicated that certain factors specific in HepG2 cells may be involved in this methylation related regulation. Biobase (http://www.biobase-international.com/) predicted possible binding of C-myc and USF to this sequence, however, qRT-PCR results showed C-myc and USF are abundant in all three cell lines (data not shown). Since there is very limited data available regarding the transcriptional regulation of CAR, the exact function of this sequence and the candidate binding proteins remain unclear.

An e-box is a special DNA sequence (CANNTG) found in some promoter regions in eukaryotes that acts as a binding site for regulating proteins (Massari and Murre, 2000). It has been reported that methylation of the CpG dinucleotide within the e-box sequence can block the binding of N-Myc to its targeting gene promoters *in vivo*, thus contributing to the cell type-specific expression pattern of certain genes, like Caspase 8 and EGFR (Perini et al., 2005). Since two e-box sequences (CACGTG) are located near the transcription start site and translation start site of CAR respectively, methylation on the CpG dinucleotide is likely to play a role in modulating CAR expression. In ourstudy, twenty-nine liver tumor samples showed decreased CYP2C19 and CAR expression along with elevated DNA methylation around the e-box binding site compared with adjacent normal liver samples. Only in sample 246564 did the situation reverse. Further scrutiny of the diagnostic information of this patient did not reveal anything unusual. Clearly, this distinct phenomenon awaits more data to be better understood. However, the reversed correlation between

CYP2C19 and CAR expression level and DNA methylation was also observed in sample 246564, which confirms the DNA methylation status might serve as a potential marker for predicting changes in gene expression.

Nevertheless, other factors cannot be excluded that contribute to the epigenetic regulation of CYP2C19 since the distal promoter region of CYP2C19 is unidentified and more transcriptional factors might exist. However, reduced CAR expression by e-box methylation at least partially account for the suppression of CYP2C19 in the HBV-infected HCC tissue samples.

It has been well documented that DNA methylation in different genomic contexts exerts different impact on gene transcription (Jones, 2012). Much attention has been paid to those CpG-rich promoters during the past years while CpG-poor transcription start sites were overlooked. In fact, non-CpG island methylation appears to be more dynamic and therefore more changeable during development or pathogenesis. For example, the CpG-poor LAMB3 promoter was shown to be hypomethylated in primary bladder tumors. *In vitro* methylation of the promoter can directly lead to transcriptional silencing (Han et al., 2011). Furthermore, enhancers, which can reside at variable distances from promoters and are mostly CpG-poor, also tend to show a variable methylation status.

Lempiäinen et al., have demonstrated that long-term activation of CAR in mice can lead to HCC, which is accompanied by a switch in the methylome (Lempiäinen et al., 2011). However, it remains controversial whether CAR plays a direct role in human HCC. The pathogenesis of cancer is a complex process in which multiple genetic and

epigenetic factors are regulated abnormally. This complexity poses a formidable challenge to holistic integration of information when investigation is limited to only a certain gene. Traditionally, epigenetic researches on cancer were mostly focused on tumor suppressors or oncogenes. Only in recent years has the necessity of building a comprehensive epigenome map been realized. Compared with the well-established Human Genome Project, the International Human Epigenome Consortium just launched in 2010, which aims at understanding how the epigenome has shaped human populations over generations, and how it is responded to the environment (http://ihec-epigenomes.org/). Goals of this project include generating high resolution maps of DNA methylation and informative histone modifications, as well as comparative analysis of epigenome maps between healthy and diseased status. It is highly anticipated that advances in the field of epigenetics will shed light on those intricate life processes such as tumorigenesis and aging.

Acknowledgements

Authorship Contributions

Research design: S. Chen, Zeng, and Tang

Sample collection: Ge, Kong, and Z Chen

Experiments conduction: Tang, Liu, and Xu

Data analysis: Tang, and Liu

Manuscript writing: Tang, S.Q. Chen, and Zeng

References

Chen H, Shen ZY, Xu W, Fan TY, Li J, Lu YF, Cheng ML and Liu J (2014)
Expression of P450 and nuclear receptors in normal and end-stage Chinese livers.
World J Gastroenterol **20**: 8681-8690

Christman JK (2002) 5-Azacytidine and 5-aza-2'-deoxycytidine as inhibitors of DNA
methylation: mechanistic studies and their implications for cancer therapy. *Oncogene*
21: 5483-5495

Griskevicius L, Yasar U, Sandberg M, Hidestrand M, Eliasson E, Tybring G, Hassan
M and Dahl ML (2003) Bioactivation of cyclophosphamide: the role of polymorphic
CYP2C enzymes. *Eur J Clin Pharmacol* **59**: 103-109.

Han H, Cortez CC, Yang X, Nichols PW, Jones PA and Liang G (2011) DNA
methylation directly silences genes with non-CpG island promoters and establishes a
nucleosome occupied promoter. *Hum Mol Genet* **20**:4299-4310.

Helsby NA, Lo WY, Sharples K, Riley G, Murray M, Spells K, Dzhelai M, Simpson
A and Findlay M (2008) CYP2C19 pharmacogenetics in advanced cancer:
compromised function independent of genotype. *Br J Cancer* **99**:1251-1255.

Herceg Z and Paliwal A (2011) Epigenetic mechanisms in hepatocellular carcinoma:

How environmental factors influence the epigenome. *Mutat Res* **727**: 55-61

Iizuka N, Oka M, Yamada-Okabe H, Mori N, Tamesa T, Okada T, Takemoto N, Tangoku A, Hamada K, Nakayama H, Miyamoto T, Uchimura S, Hamamoto Y (2002) Comparison of gene expression profiles between hepatitis B virus- and hepatitis C virus-infected hepatocellular carcinoma by oligonucleotide microarray data on the basis of a supervised learning method. *Cancer Res* **62**:3939–3944

Ingelman-Sundberg M, Sim SC, Gomez A and Rodriguez-Antona C (2007) Influence of cytochrome P450 polymorphisms on drug therapies: pharmacogenetic, pharmacoepigenetic and clinical aspects. *Pharmacol Ther* **116**: 496-526.

Jemal A, Bray F, Center MM, Ferlay J, Ward E and Forman D (2011) Global cancer statistics. *CA Cancer J Clin* **61**: 69–90.

Ji X, Zhang Q, Du Y, Liu W, Li Z, Hou X and Cao G (2014) Somatic Mutations, Viral Integration and Epigenetic Modification in the Evolution of Hepatitis B Virus-Induced Hepatocellular Carcinoma. *Curr Genomics* **15**: 469-480.

Jones PA (2012) Functions of DNA methylation: islands, start sites, gene bodies and beyond. *Nat Rev Genet* **13**: 484-92.

Klug M and Rehli M (2006) Functional analysis of promoter CpG methylation using a CpG-free luciferase reporter vector. *Epigenetics* **1**: 127-30.

Lempiäinen H, Müller A, Brasa S, Teo SS, Roloff TC, Morawiec L, Zamurovic N, Vicart A, Funhoff E, Couttet P, Schübeler D, Grenet O, Marlowe J, Moggs J and Terranova R (2011) Phenobarbital Mediates an Epigenetic Switch at the Constitutive Androstane Receptor (CAR) Target Gene Cyp2b10 in the Liver of B6C3F1 Mice. *PLoS One* **6**: e18216

Lessel D, Vaz B, Halder S, Lockhart PJ, Marinovic-Terzic I, Lopez-Mosqueda J, Philipp M, Sim JC, Smith KR, Oehler J, Cabrera E, Freire R, Pope K, Nahid A, Norris F, Leventer RJ, Delatycki MB, Barbi G, von Ameln S, Högel J, Degoricija M, Fertig R, Burkhalter MD, Hofmann K, Thiele H, Altmüller J, Nürnberg G, Nürnberg P, Bahlo M, Martin GM, Aalfs CM, Oshima J, Terzic J, Amor DJ, Dikic I, Ramadan K and Kubisch C (2014) Mutations in SPRTN cause early onset hepatocellular carcinoma, genomic instability and progeroid features. *Nat Genet* **46**: 1239-1244.

Massari ME and Murre C (2000) Helix-loop-helix proteins: regulators of transcription in eucaryotic organisms. *Mol Cell Biol* **20**: 429-440.

Nishida N and Goel A (2011) Genetic and epigenetic signatures in human hepatocellular carcinoma: a systematic review. *Curr Genomics* **12**: 130–137.

Okabe H, Satoh S, Kato T, Kitahara O, Yanagawa R, Yamaoka Y, Tsunoda T, Furukawa Y, Nakamura Y (2001) Genome-wide analysis of gene expression in human hepatocellular carcinomas using cDNA microarray: identification of genes involved in viral carcinogenesis and tumor progression. *Cancer Res* **61**:2129–2137

Perini G, Diolaiti D, Porro A and Della Valle G (2005) In vivo transcriptional regulation of N-Myc target genes is controlled by E-box methylation. *Proc Natl Acad Sci USA* **102**: 12117-12122.

Schmittgen TD and Livak KJ (2008) Analyzing real-time PCR data by the comparative C_T method. *Nat Protoc* **3**:1101-1108.

Shou M, Martinet M, Korzekwa KR, Krausz KW, Gonzalez FJ, Gelboin HV (1998) Role of human cytochrome P450 3A4 and 3A5 in the metabolism of taxotere and its derivatives: enzyme specificity, interindividual distribution and metabolic contribution in human liver. *Pharmacogenetics* **8**: 391-401

Thorgeirsson SS and Grisham JW (2002) Molecular pathogenesis of human hepatocellular carcinoma. *Nat Genet* **31**: 339-346.

Tsunedomi R, Iizuka N, Hamamoto Y, Uchimura S, Miyamoto T, Tamesa T, Okada T,

Takemoto N, Takashima M, Sakamoto K, Hamada K, Yamada-Okabe H and Oka M

(2005) Patterns of expression of cytochrome P450 genes in progression of hepatitis C

virus-associated hepatocellular carcinoma. *Int J Oncol* **27**: 661-667.

Uppugunduri CR, Daali Y, Desmeules J, Dayer P, Krajinovic M and Ansari M (2012)

Transcriptional Regulation of CYP2C19 and its Role in Altered Enzyme Activity.

Curr Drug Metab **13**: 1196-1204.

Wortham M, Czerwinski M, He L, Parkinson A and Wan YJ (2007) Expression of

Constitutive Androstane Receptor, Hepatic Nuclear Factor 4α, and P450

Oxidoreductase Genes Determines Interindividual Variability in Basal Expression and

Activity of a Broad Scope of Xenobiotic Metabolism Genes in the Human Liver.

Drug Metab Dispos **35**: 1700-1710.

Yu D, Green B, Tolleson WH, Jin Y, Mei N, Guo Y, Deng H, Pogribny I, Ning B

(2015) MicroRNA hsa-miR-29a-3p modulates CYP2C19 in human liver cells.

Biochem Pharmacol **98**: 215-223

Footnotes

Legends for Figures

Figure 1. Location of the sequences examined by BSP, MSP and reporter gene assay. CpG sites are shown as vertical bars with dots. Transcription start sites (TSS) are shown as curved arrows and are marked as position +1. E-box binding sites are pointed by down arrows. Double-arrow bars indicate sequences examined by BSP and the capped line indicates sequence examined by MSP. Sequence in box indicates CpG island identified by Methyl Primer Express® Software v1.0 (ABI, Foster City, CA). The sequences analyzed by reporter gene assay are shown as horizontal thick lines marked with starting and ending position.

Figure 2. Maps of the CpG-free vectors used in the reporter gene assay.

Figure 3. Expression profiles of CYP2C19 and related transcriptional factors in primary hepatocytes after 5-aza-dC treatment. The relative expression of CYP2C19, CAR, GATA-4, HNF-3γ, PXR, GRα and HNF-4α are shown as mean ± S.E. $p*<0.05$. X-axis indicates the concentration of 5-aza-dC. Data are from 4 independent experiments of 2 donors.

Figure 4. DNA methylation of CpG sites in (a) segment 1, 2 and 3 on the promoter region of CYP2C19, (b) segment 5 near the CAR transcription start site, (c) segment 6 near the CAR translation start site, (d) segment 4 on the promoter region of CAR. CpG sites of the control group and 1μM 5-aza-dC treated group are shown as red

circles and green triangles, respectively. Data are representative of the female donor.

Figure 5. Relative expression of CYP2C19 and CAR in 30 HCC tumorous tissues compared with matched adjacent normal tissues. (a) Comparison of CYP2C19 and CAR expression in matched HCC tumorous tissues and adjacent normal tissues by Paired Student's t test. Data are shown as scatter plots with mean± S.E., p***<0.001. (b) Representative CYP2C19 and CAR expression in matched HCC tumorous tissues (C) and adjacent normal tissues (N). Data are shown as mean. (c) The Pearson correlation between mRNA expression of CYP2C19 and CAR.

Figure 6 Methylation analysis of segment 5 near the CAR transcription start site. (a) Comparison of methylation status of CpG sites within segment 5 between HCC tumorous tissues (red circles) and adjacent normal tissues (green triangles). (b) MSP analysis of the e-box binding site within segment 5. DNA samples from tumorous and normal tissue are shown as C and N. Segment 5 amplified by PCR was used as either methylated control DNA (Me, M. SssI treated) or unmethylated control DNA (Un). Methylation-specific primers are shown as M and unmethylation-specific primers are shown as U.

Figure 7 Effect of DNA methylation on the transcriptional activity of CYP2C19 and CAR promoter constructs. (a, c, d) The pCpGL plasmids were co-transfected with pRL-TK in HepG2, HEK293 or HK2 cells. The pCpGL plasmids were either

methylated in the presence (methylated) or absence of (unmethylated) M. SssI. (b)

The CpGfree constructs were co-transfected with pCpGL-2C19 and pRL-TK in

HepG2 cells. The CpGfree constructs were either methylated in the presence

(methylated) or absence of (unmethylated) M. SssI. The relative luciferase activity

was calculated as ratio of firefly luciferase to Renilla luciferase. Data are shown as

mean ± S.D. with 3 replicate wells for each group. Data are representative of 3

independent experiments. $p^{**} < 0.01$.

Table 1 Primer sequences for qRT-PCR

	Accession No.*	Forward primer (5'-3')	Reverse primer (5'-3')
CYP2C19	NM_000769.2	GAAAAATTGAATGAAAACATCAGGATTG	CGAGGGTTGTTGATGTCCATC
CAR	NM_005122.4	GCAGCTGTGGAAATCTGTCA	CAGGTCGGTCAGGAGAGAAG
GRα	NM_000176.2	GGGGAAGAGGGAGATGGA	GTGGTCAGAATGGGAGGC
PXR	NM_022002.2 NM_033013.2	CAAGCGGAAGAAAAGTGAACG	CTGGTCCTCGATGGGCAAGTC
	NM_003889.3		
GATA-4	NM_001308094.1	CTGGCCTGTCATCTCACTACG	GGTCCGTGCAGGAATTTGAGG
	NM_001308093.1		
	NM_002052.4		
HNF-3γ	NM_004497.2	ATGCTGGGCTCAGTGAAGAT	CAGGTAGCAGCCATTCTCAA
HNF-4α	NM_178849.2	GGTCAGGTGGGGTGGATGATATAATG	TCTAGGTTAATAGGGAGGAAGGGAGG
	NM_178850.2		

33

	NM_001258355.1		
GAPDH	NM_002046.5	GAAGGTGAAGGTCGGAGTC	CAAAGTTGTCATGGATGACC
	NM_001289745.1		
	NM_001289746.1		

Primers were designed to amplify either all transcription variants or variants that predominate in liver.

34

Table 2 Primer sequences for BSP and MSP

	Gene ID	Forward primer (5'-3')	Reverse primer (5'-3')
Primers for BSP			
CYP2C19 segment 1	1557	GGTAGTATATTTTTGTTAGAGTTTAAAG	AATCCACAAATATTTACTAATTATATACA
CYP2C19 segment 2	1557	GAGAATTGGAAATAATTTTATTAGG	ACCACCACAATATATAAACCTTAAC
CYP2C19 segment 3	1557	GTTTTGTTTTGTTAAAATAAAGTTTTAGT	AACCCAAATAATTCCAATACACC
CAR segment 4	9970	GTAAATGAAGAAGTAGAAGATATAATAG	AATAACTCATACCTATAATCCCAACA
CAR segment 5	9970	TAGTTATTGAGAGTAATTGGAGGTTATA	CCTTAACTTCCCAAAATACTAAAATTACA
CAR segment 6	9970	TTAGAAGGGATAGAAAAGGGTTAAGG	ACTATATCCATCAAACAAACATTCAAC
Primers for MSP			
CAR-MSP-M	9970	GTTGGGGGTTAGGTATAGTGGTTTACGA	CTAAAATTACAAACATAAACTCCCGCGT
CAR-MSP-U	9970	TTGGGGGTTAGGTATAGTGGTTTATGA	TACTAAAATTACAAACATAAACTCCCACAT

Table 3 Primer sequences for plasmids construction

	Gene ID	Forward primer (5'-3')	Reverse primer (5'-3')
pCpGL-CYP2C19	1557	GGactagtATTATTCTAAAGAGAGCAAC	CGggatccTTAAGACAACCGTGAG
pCpGL-CAR-2E	9970	GGactagtGAAATCTGTTGGGGACCAAAGACTAA	CGggatccCTGTGTCCATCAGACAAACATTCAG
pCpGL-CAR-1E	9970	GGactagtCCTGTAATCCCAGCACTTTGGGAAGCC	CGggatccCTGTGTCCATCAGACAAACATTCAG
pCpGfree-CAR	9970	Flanking-F	Flanking-R
		GGactcgtCTCTCTCTCTCTCTTCCCAGCTTG*	<u>TACTGGCCATGACGTCACG</u>TGTTGGG
	NM_005122.4	CDS-F	CDS-R GAagatctCCTCAGCTGCAGATCTCCTGGA
		<u>CGTGACGTCATGGCCAGTA</u>GGGAAGATGAG	

*Lower-case letters indicated the added restriction sites; underlined letters indicated the overlapping part of the primers for overlap PCR.

36

Figure 1

CYP2C19

Segment 1
Segment 2
Segment 3

TSS(+1)

pCpGL-CYP2C19   (-1977)   (+64)

CAR

TSS(+1)   E-box(+247)   E-box(+1637)

CpG island

Segment 4
Segment 5
Segment 6

pCpGL-CAR-CGI   (-1446)   (+1971)

pCpGL-CAR-2E   (+175)   (+1971)

pCpGL-CAR-1E   (+384)   (+1971)
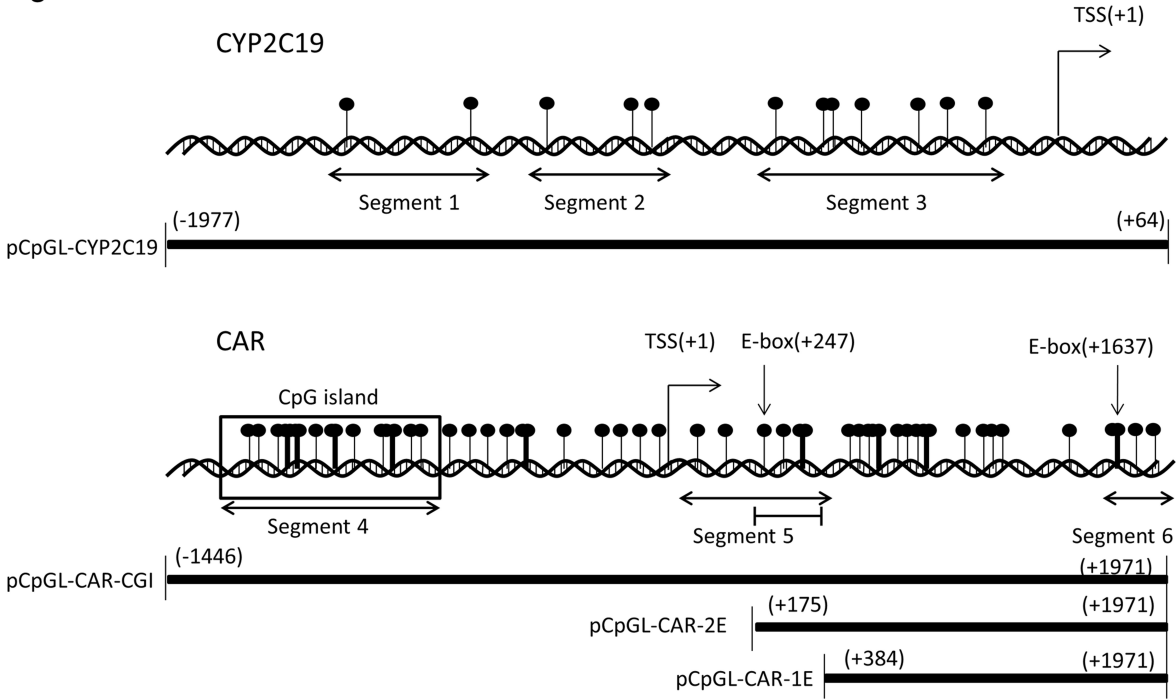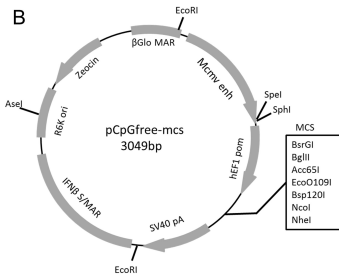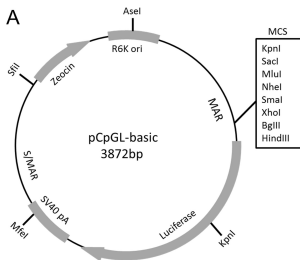
Figure 2

Figure 3

Figure 4

Figure 5

A

CYP2C19

CAR

B

C

Correlation of CYP2C19 and CAR expression

R^2=0.095
p*=0.0169

Figure 6

Figure 7